JOURNAL OF EXPERIMENTAL AND THEORETICAL PHYSICS, 2024, Vol. 165, No. 1, pp. 69–83

NUCLEATION IN A NON-IDEAL RAPIDLY COOLING VAPOR

© 2024 *E. E. Perevoshchikov, D. I. Zhukhovitskii*[*]

Joint Institute of High Temperatures of the Russian Academy of Sciences

125412, Moscow, Russia

Abstract. The problem of non-stationary vapor-liquid nucleation is solved at a constant number of particles and a fixed cooling rate. An analytical approach to solving kinetic equations is developed, which correctly takes into account both the dependence of the work of cluster formation on its size and the non-ideality of the condensing vapor. Comparison with a similar approach based on the classical model reveals qualitative differences in the results. To assess the correctness of various approaches, simulation of the process under consideration was performed using the molecular dynamics method, the results of which are in qualitative and quantitative agreement with the proposed analytical model and are in much worse agreement with other approaches. Estimates for silicon oxide nucleation indicate that the significant d ifference b etween t he e quation o f s tate o f c ondensing v apor and the ideal gas equation may be its universal property.

DOI: 10.31857/S00444510240108e1

1. INTRODUCTION

The input of high energy density into condensed matter results in the formation of regions where it rapidly expands and turns into dense vapor. The vapor then cools, which leads to nucleation with the formation of liquid or solid microparticles. Examples include laser evaporation [1, 2], ablation of matter into vacuum [3, 4] and liquid [5, 6], and the formation and evolution of regolith during the collision of micrometeorites with the lunar surface [7].

In these and a number of other cases, the system quickly passes through the binodal and moves toward the spinodal until a "condensation explosion" occurs, i.e., a violent release of microdroplets-nuclei of the liquid phase, which transfers the system to a state approaching quasi-stationary. With a further drop in temperature, "freezing" of the condensation process is possible [7]. The presence in the cooling vapor of centers that attract monomers of the condensing vapor, in particular, ions, leads to a more complicated picture of the process compared to the case of homogeneous nucleation occurring in the absence of impurities. However, even the theory of homogeneous nucleation is currently far from complete due to such objective difficulties as the need to describe cluster objects containing several dozen monomers, taking into account the non-ideality of the condensing vapor, the non-isothermality of the clusters, the non-stationarity of the flow of the resulting supercritical clusters, which are embryos of the liquid phase, etc. The theoretical description of the "condensation explosion" is based on the theory of stationary homogeneous nucleation and modeling the kinetics of non-stationary nucleation.

In the classical nucleation theory (CNT) [8–10], a number of assumptions are made that limit its applicability. Thus, a macroscopic interfacial tension σ is assigned to the cluster surface, although it is not obvious that macroscopic equilibrium quantities are applicable to the description of a typical critical cluster of about 50 particles (monomers). Modern theoretical approaches [11–16] and experimental results in a number of cases are in poor agreement [17–19].

In the works [20–27], a two-parameter model (TPM) of "hot" clusters at temperatures between the melting point and the critical point was proposed and developed. It is based on the idea that the lightest clusters are a system of virtual chains, and a cluster of arbitrary size is a core with properties close to those of a liquid, surrounded by a layer of particles in almost the same state as in the lightest clusters. In particular, it was shown that the effective surface tension of small clusters differs significantly from this value for a flat surface (see, e.g., [20]).

The theory of nucleation based on classical assumptions limits the kinetic paths of cluster evolution to condensation and evaporation of individual particles only. However, in some systems, processes such as fusion and fragmentation of entire clusters cannot be excluded from consideration. This is especially true for dense systems located near the point of the "condensation explosion", where the clusters in question acquire a fractal structure [27].

[*] E-mail: dmr@ihed.ras.ru

Numerical simulation is a traditional approach to studying non-stationary nucleation; molecular dynamics (MD) [28–37] and Monte Carlo [38–41] methods are used. Nucleation simulation requires ensembles of a large number of particles (at least 10^6), and is computationally intensive. Therefore, the development of highly efficient analytical approaches to solving this problem is very important, especially since these approaches are not sufficiently developed. In [7], an approximate solution to the problem of explosive nucleation during rapid adiabatic expansion of vapor into vacuum was found, and in [42, 43], using the same method, explosive nucleation was studied at given temperature and vapor pressure as functions of time. In the above-mentioned works, vapor was considered as an ideal gas. However, already from the formulation of the cluster vapor model [21, 26], in which a mixture of ideal gases of the lightest clusters is considered, it follows that this is, generally speaking, not the case.

In this paper, the analytical approach [42] is modified to take into account both the correct size dependence of the cluster formation work and the non-ideality of the condensing vapor. It turns out that the second factor has a more significant effect on the explosive nucleation process than the first, and the non-ideality effect is quite significant at both low and high supersaturations at the moment of explosive nucleation. Taking this effect into account leads to a qualitative difference from the most commonly used theories of nucleation, since it predicts a "condensation explosion" in the metastable region, whereas if non-ideality were not taken into account, the system would have to be in the region of lability.

The non-ideality of condensing vapor was discussed in [44], where it was first pointed out that the rate of formation of liquid-phase nuclei from supersaturated vapor is determined not by the ratio of the actual vapor pressure to the saturation pressure, but by the ratio of the partial pressure of monomers in the supersaturated vapor to their partial pressure on the binodal at the same temperature. Since the vapor becomes non-ideal due to the formation of clusters in it, the second ratio turns out to be noticeably smaller than the first. However, specific methods for calculating the partial pressure of monomers are not discussed in this work. Such a method was proposed in [45], where the equation of state of non-ideal vapor was described using virial expansion. However, since direct calculation of the integrals determining the virial coefficients encounters significant difficulties, the authors introduce an additional free parameter determined from the best fit to experiment. Note that in the model used in this work, the introduction of an additional parameter is not required, since the equation of state of a non-ideal vapor is modeled on the basis of the TPM using the same parameters that determine the dimensional correction to the work of cluster formation and, in principle, can be taken from independent sources.

In this work, MD simulation of non-stationary nucleation in a Lennard-Jones system was carried out under conditions where the rate of formation of supercritical clusters can be considered quasi-stationary, which made it possible to compare the results of MD simulation with the results of the analytical approach proposed in the work and demonstrate their satisfactory agreement.

In Section 2 the basic principles of the cluster vapor model based on the TPM are formulated, which allows one to calculate the compressibility factor of a non-ideal vapor (to obtain its equation of state). The procedure for simulation of the "condensation explosion" in the Lennard-Jones system, as well as the simulation results, are discussed in Section 3. The analytical theory of the "condensation explosion", taking into account the non-ideality of the vapor, is presented in Section 4, and the results of calculations based on it and a comparison with MD simulation, as well as the results of calculations for silicon oxide, are presented in Section 5. The main conclusions are formulated in Section 6.

2. CLUSTER VAPOR MODEL

The non-ideality of the condensing vapor means that the average potential energy of interaction of the monomers cannot be neglected in comparison with their average kinetic energy. In this paper, we consider a homogeneous system in which both the gas and liquid phases are formed by the same stable molecules, which are considered monomers (particles). The interaction of monomers can lead to the formation of their bound states, called clusters, the average residence time in which for a monomer is much greater than the ratio of the characteristic length of action of interparticle forces to the thermal velocity of the monomer. The interaction between the monomers that form each cluster will be called bound interaction, and the remaining types of interaction, free interactions. The latter, therefore, include interactions between monomers that are not part of clusters, between these monomers and clusters, and between different clusters. A situation is possible when the average energy of bound interaction significantly exceeds the average

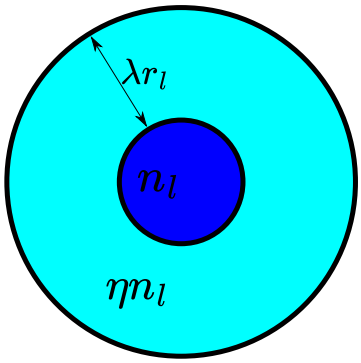

Fig. 1. Cluster model

energy of free interactions, with the latter being much less than the average kinetic energy of the monomers. Then we can neglect the energy of free interactions, considering that all interactions of monomers are reduced to the formation of molecular clusters, and treat a mixture of ideal gases of monomers and clusters, in which reactions of the form $A_k + A_l \rightleftarrows A_{k+l}$ occur, where A_k denotes a cluster consisting of k monomers; $k, l = 1, 2, \ldots$. In this case, the vapor as a whole turns out to be non-ideal. The described vapor model was first proposed in [46, 47], and then used in various studies (e.g., [26, 44]). Its applicability in the supersaturated vapor region is beyond doubt, since the cluster number density there increases infinitely with increasing supersaturation, and on the binodal and in the unsaturated vapor region it is verified by the agreement between model calculations and experiment, including numerical one [26, 27]. The approach to describing the non-ideality of a vapor, proposed by the model of a mixture of ideal gases of clusters, does not contradict the method of virial expansion in powers of vapor density, since it is possible to establish a unique correspondence between the coefficients of virial expansion and the equilibrium constants of reactions of formation of clusters of different sizes. At the same time, although virial expansion is a more general approach, taking into account both bound and free interactions, direct calculation of virial coefficients in a system containing clusters encounters significant difficulties.

Let us consider the vapor as an ideal mixture of clusters of different sizes k, the actual number density of which we denote by n_k, and the equilibrium number density $\bar{n}_k$. The clusters themselves are considered to consist of a core similar to a continuous liquid, and a surface layer similar to a system of virtual chains. A schematic illustration of such a cluster model is shown in Fig. 1. The surface energy of a cluster is proportional not to the surface area, but to the number of particles in the surface layer k_0 of a cluster containing k particles (we will also refer this number as the cluster size). Then, as was shown in the works [21, 48],

$$\begin{aligned} &\text{at } k \geq (\lambda^2/2)(\lambda + 2\delta) \\ &\quad k_0 = 3\eta\lambda(k-k_0)^{2/3} + 3\eta\lambda^2(k-k_0)^{1/3} + \eta\lambda^3, \\ &\text{and when } k < (\lambda^2/2)(\lambda + 2\delta) \\ &\quad k_0 = k, \end{aligned} \tag{1}$$

where the dimensionless parameters of the TPM δ and λ are introduced, so that $r_\ell\delta$ and $r_\ell\lambda$ are the Tolman length and the thickness of the surface layer of the cluster, respectively; $\eta = \delta/\lambda + 1/2$; $r_\ell = (3/4\pi n_\ell)^{1/3}$ is the characteristic size of the molecular cell in the liquid, n_ℓ is the number density of particles in the cluster core, which coincides with the number density in the bulk liquid phase; ηn_ℓ is the number density of particles in the surface layer (Fig. 1). In this case, the work of formation of a k-particle cluster can be written as [21]

$$\Delta\Phi_k = (k_0 - 1)T\ln(Kn_{1s}) - (k-1)T\ln(S), \tag{2}$$

where $S = n_1/n_{1s}$ is the vapor supersaturation, n_1 is the monomer number density, T is the temperature in energy units; here and below, the quantities with subscript s refer to the saturation line. Within the framework of the cluster vapor model used, S can also be represented as the ratio of the partial pressures of the monomers in the nonequilibrium state and on the saturation line at the same temperature. However, S differs from the ratio of the vapor pressure to the saturation pressure the more, the greater the degree of vapor non-ideality. Since the nucleation rate defining the nucleation kinetics, which is equal to the number of supercritical embryos formed in a unit volume per unit time, is extremely sensitive to S, the vapor non-ideality significantly affects, first of all, the nucleation rate.

Introducing the relationship between the dimer equilibrium constant $K(T) = n_2/n_1^2$ and the macroscopic surface tension σ [21]

$$\kappa(T) = \exp\left[-\frac{8\pi\sigma r_\ell^2}{3(\lambda + 2\delta)T}\right] = Kn_{1s}, \tag{3}$$

we can transform (2) to the form

$$\Delta\Phi_k = 4\pi\sigma r_\ell^2\gamma_k k^{2/3} - (k-1)T\ln(S), \tag{4}$$

where

$$\gamma_k = \frac{2(k_0 - 1)}{3(\lambda + 2\delta)k^{2/3}}. \tag{5}$$

The expression for the minimum work of cluster formation can be used to obtain the equilibrium distribution of clusters by size

$$\bar{n}_k = n_1 \exp\left[-\frac{\Delta\Phi_k}{T}\right]. \tag{6}$$

Since it is assumed that only small, close to equilibrium clusters of size $k < 10$ contribute to the equation of state, taking into account (1) we have

$$\bar{n}_k = n_1^k K^{k-1}, \tag{7}$$

which allows us to calculate the compressibility factor far from the critical point, i.e. to obtain the equation of state of the cluster vapor [21]

$$Z = \frac{\sum_{k=1}^{\infty} n_k}{\sum_{k=1}^{\infty} k n_k} \simeq 1 - \kappa S. \tag{8}$$

From (8) it is clear that, firstly, always $Z < 1$, which is typical for the used model of a cluster vapor, and, secondly, for any $\kappa > 0$ the vapor becomes increasingly non-ideal with the growth of S. Thus, the non-ideality of the vapor is greater, the further the system enters the metastable region.

The distribution of clusters in a supersaturated vapor whose size is of the order of or greater than the critical one g is nonequilibrium, and a flow of clusters capable of unlimited growth equal to the nucleation rate appears in the size space. Its calculation within the TPM framework leads to the expression [21]

$$\begin{aligned} I_{TPM} &= \alpha n_{vs}^2 r_\ell^2 v\pi \frac{S^2 Z_s^4}{Z^{3/2}\eta^{2/3}} \\ &\times \left[\sum_{k=1}^{\infty} k^{-2/3} \exp\left(\frac{\Delta\Phi_k}{T}\right)\right]^{-1} \\ &\simeq \frac{\alpha n_{vs}^2 S Z_s^4}{n_\ell \eta^{2/3} Z^{3/2}} \left(\frac{2\sigma}{\pi m}\right)^{1/2} e^{-(3\gamma_{g_{TPM}}-2)\Phi_*}, \end{aligned} \tag{9}$$

where $\alpha \approx 1$ is the accommodation coefficient, n_v is the vapor density, m is the mass of the monomer, $v = \sqrt{8T/\pi m}$ is its thermal velocity, g_{TPM} is the critical size of the embryo in the TPM, $\Phi_* = (16\pi/3)(\sigma^3/n_\ell^2 T^3 \ln^2 S)$ is the work of cluster formation in CNT.

Neglecting the dependence of the cluster surface tension on its size is equivalent to substituting $\gamma_k \equiv 1$ into (4). Then, neglecting the non-ideality of the vapor, the expression (9) reduces to the classical Zeldovich formula in CNT [8]:

$$I_{CNT} = \sqrt{\frac{2\sigma}{\pi m}} \frac{n_v^2}{n_\ell} e^{\Phi_*}, \tag{10}$$

and the expression for the critical size of the embryo in the CNT can be written as

$$g_{CNT} = \frac{2\Phi_*}{\ln S}. \tag{11}$$

The critical size g_{TPM} can be expressed in terms of g_{CNT}:

$$\begin{aligned} g_{TPM} &= \frac{1}{2}(\lambda + 2\delta)\left(3g_c^{2/3} + 3\lambda g_c^{1/3} + \lambda^2\right) + g_c, \\ g_c &= \lambda^3 \left(\sqrt{1 + \frac{2\lambda}{g_{CNT}^{1/3} - \lambda - 2\delta}} - 1\right)^{-3}. \end{aligned} \tag{12}$$

An alternative to the TPM is the self-consistent classical nucleation theory (SCCNT), in which, due to the introduction of the correction factor $A = \exp(-4\pi\sigma r_\ell^2/T)$, the work of monomer formation turns out to be zero. This is equivalent to substituting $\gamma_k = (k^{2/3} - 1)k^{-2/3}$ into (4). In this case, the nucleation rate I_{SCCNT} is equal to

$$I_{SCCNT} = A I_{CNT}, \tag{13}$$

and the critical size is still expressed by formula (11).

3. NUMERICAL SIMULATION

3.1. Simulation procedure

For numerical simulation of the nucleation process during rapid cooling of the Lennard-Jones system, we use the molecular dynamics method. The MD simulation was carried out using the LAMMPS [49] software package. The interaction of two particles at a distance r is described by the Lennard-Jones potential with a cutoff and a shift

$$\begin{aligned} u(r) &= \begin{cases} w(r) - w(r_c), & r \le r_c, \\ 0, & r > r_c, \end{cases} \\ w(r) &= 4\epsilon\left[\left(\frac{a}{r}\right)^{12} - \left(\frac{a}{r}\right)^{6}\right], \end{aligned} \tag{14}$$

where ϵ is the depth of the potential well, a is the distance at which the interaction energy becomes zero, $r_c = 2.5a$ is the cutoff radius. Further, the quantities will be given in dimensionless units with the scales $\tau_0 = a\sqrt{m/24\epsilon}$ in time, where m is the mass of the particles forming the system; a is the distance; ϵ is the energy and temperature. It follows from the definition of these scales that when substituting dimensionless quantities into the formulas, the result will also be dimensionless if we set $m = 24$. Periodic boundary conditions are set in three directions of the cubic cell; a

Langevin thermostat with a time relaxation parameter of 1000 time steps is used to control the temperature. In molecular dynamics, a thermostat is an analogue of a carrier gas that ensures temperature equalization in a real process. The calculation is performed with a time step of 0.005.

The number of particles in the system N was chosen equal to 10^6. As test calculations showed, in which N varied from 10^5 to 10^6, the dependence of all the simulation results on N, and in particular the maximum cluster size in the system, on this number almost disappears.

The total number of particles in the system N in this simulation was constant, and the total number of particles per unit volume n_{v0} (the total number density), which did not change in each run, depended on the size of the simulation cell $L = \sqrt[3]{N/n_{v0}}$. In the calculations performed, this value varied from 319.1 to 351.2. The temperature in the initial state T_0 was specified as $T_0 = 1.1T_s(n_{v0})$, i.e. it corresponded to the equilibrium gas above the binodal. The system was maintained in this state for some time until it reached equilibrium, after which there followed a stage of cooling the system according to the established linear law $T(t) = T_0 - \xi(t + t_b)$, where ξ is the cooling rate, which varied from 1.4×10^{-6} to 10^{-5}, t_b is the time to reach the binodal from the initial state; time is counted from the moment of crossing the binodal.

This simulation does not take into account the change in the number of particles per unit volume n_v that occurs during expansion of the vapor cloud or during nucleation in the flow. However, as shown in [42], the "condensation explosion" occurs so quickly that during its characteristic time the vapor density changes little, and this change, unlike the change in temperature, does not fundamentally affect the quantities characterizing the point of the "condensation explosion".

To obtain the distribution of clusters by size, the following definition of a cluster is used: two particles belong to one cluster if there is a continuous chain of particles between them, the distance between which is less than $r_b = 1.5$, while one particle cannot simultaneously belong to two clusters. According to the definition, a particle that does not have neighbors at a distance less than r_b is a separate cluster, i.e. a monomer. Based on this definition, cluster analysis was performed to obtain the distribution of the numbers of clusters by their sizes N_k, from which the number density of clusters $n_k = N_k/L^3$ was calculated.

The vapor density in a nonequilibrium two-phase system can be defined as the total number density of particles belonging to subcritical clusters

$$n_v = \sum_{k=1}^{g} k n_k. \tag{15}$$

In this case, the liquid phase is treated as a dispersed system of supercritical clusters (droplets). However, this definition requires knowledge of the critical cluster size g, which is unknown from molecular dynamics. In the works [21, 26] it was shown that the main contribution to compressibility is made by small clusters with sizes $k_m \lesssim 10$. Therefore, in (15), summation up to the critical size g can be replaced by summation up to some size k_m. The value of k_m changes slightly under different conditions, and it can be estimated on the saturation line from the relation

$$\sum_{k=1}^{k_m} k n_k = \epsilon_g n_{vs}, \quad \epsilon_g = 0.9, \tag{16}$$

where k_m weakly depends on $\epsilon_g \lesssim 1$. Thus,

$$n_v \approx \sum_{k=1}^{k_m} k n_k. \tag{17}$$

Let us introduce the "density" supersaturation $S_\rho = n_v/n_{vs}$ and establish its connection with S. According to [21]

$$n_v = \frac{n_1}{(1-\kappa S)^2}, \quad n_{vs} = \frac{n_{1s}}{(1-\kappa)^2}, \tag{18}$$

from which follows the desired relationship, illustrated for different values of κ in Fig. 2.

$$\begin{gathered} S_\rho = S\left(\frac{1-\kappa}{1-\kappa S}\right)^2 = S\frac{Z_s^2}{Z^2} = \nu S, \quad \nu = \frac{Z_s^2}{Z^2}, \\ S = \frac{\kappa + \beta - \sqrt{2\kappa\beta + \beta^2}}{\kappa^2}, \quad \beta = \frac{(1-\kappa)^2}{2S_\rho}. \end{gathered} \tag{19}$$

From Fig. 2 it is evident that in the case where the non-ideality of the vapor is significant ($\kappa = 0.1$), the growth of S noticeably lags behind the growth of S_ρ due to the deficiency of monomers in the metastable vapor.

To calculate the density supersaturation S_ρ and the true supersaturation S, the thermophysical properties of the Lennard-Jones system are required, as well as the values of the TPM parameters determined for the interparticle interaction potential (14) with a cutoff radius of 2.5 used in this work. Such thermophysical properties are given in the works [21, 50]. They were interpolated by the following dependencies:

$$\begin{aligned} n_\ell &= -0.2166T^2 - 0.2534T + 1.0617, \\ \sigma &= -1.811T + 1.852, \\ n_{vs} &= 40.710\exp\left(-q/T\right), \quad q = 6.090. \end{aligned} \tag{20}$$

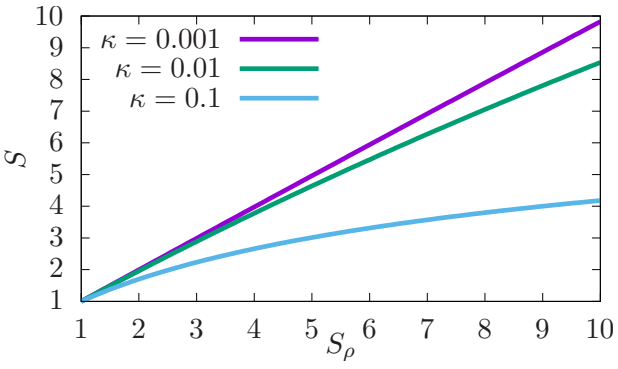

Fig. 2. Dependence of S on S_ρ for different κ

From the form of the approximation n_{vs} it follows that $q = T^2\,(d\ln n_{vs}/dT)$ is the heat of evaporation for the Lennard-Jones system. Since the vapor on the saturation line is slightly non-ideal, we will also assume in what follows that $q \simeq T^2\,(d\ln n_{1s}/dT)$. The TPM parameters for the potential (14) were borrowed from [21]: the dimensionless Tolman length $\delta = -0.07$ and the dimensionless thickness of the cluster surface layer $\lambda = 2.1$.

The value of S_ρ was calculated from the MD simulation data using (17) and the n_{vs} approximation (20), and the value of S was calculated using the relations (19), thermodynamic data (20), and the definition of κ (3). The position of the maximum of S_ρ during cooling of the system depends weakly on k_m, which allows one to determine the temperature at the nucleation point with high accuracy and to obtain an estimate of the critical size g from the analytical dependences (12) using (19).

The degree of condensation x is determined by the total number of particles in supercritical clusters, divided by the total number of particles in the system

$$x = \sum_{k=g}^{\infty} \frac{kN_k}{N} = 1 - \sum_{k=1}^{g-1} \frac{kn_k}{n_{v0}} \approx 1 - n_{v0}^{-1} \sum_{k=1}^{k_m} kn_k. \quad (21)$$

Also important for practical application is the number density of the formed droplets n_d, which, according to molecular dynamics data at the moment of reaching maximum supersaturation t^S_{max} can be determined as

$$n_d = \sum_{k=g}^{\infty} n_k. \quad (22)$$

3.2. Simulation results

An isochorically cooled system initially reaches the saturation line, where supersaturation is by definition

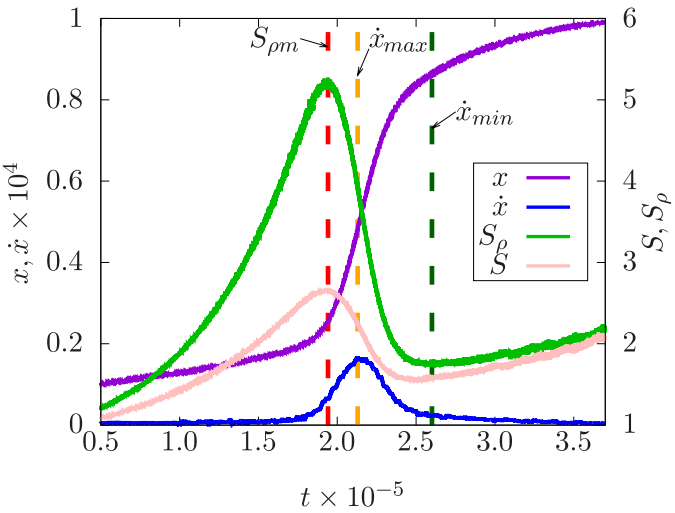

Fig. 3. Evolution of the main parameters of the system during MD simulation. $\xi = 10^{-6}, n_{v0} = 3/130$

equal to unity. The behavior of the main parameters at later moments in time is shown in Fig. 3. It is seen that the supersaturation of the vapor continues to grow and reaches its maximum value $S_{\rho m} = S_\rho\,(t_m)$. At this point, the most intense formation of supercritical nuclei occurs. Then the supersaturation drops sharply, and the rate of change of the degree of condensation $\dot{x}_{max} = \dot{x}\,(t^x_{max})$ reaches its maximum, when the condensation of particles on the already formed nuclei is the determining process. After this, at $t > t^x_{st}$, the degree of condensation almost reaches a stationary value ($\dot{x}_{st} \approx \dot{x}\,(t^x_{st})$, in Fig. 3, the moment t^x_{st} is denoted by the symbol $\dot{x}_{min}$). It can be noted that at $t > t^x_{st}$ supersaturation starts to grow again. This is due to the fact that in a system where almost all the substance is in the liquid phase, the vapor number density is low. At the same time, the rate of its condensation on the formed clusters also decreases, i.e. this process is "frozen", while the saturation pressure decreases sharply with a drop in temperature. Note that the evolution of the true supersaturation S qualitatively repeats the evolution of S_ρ (Fig. 3).

Since the dependence $\dot{x}(t)$ is well described by the Gaussian curve, the moment in time t^x_{st} can be defined as being $3\sigma_x$ away from t^x_{max}, where σ_x is the standard deviation for the corresponding Gaussian curve:

$$t^x_{st} = t^x_{max} + 3\sigma_x, \quad \sigma_x = \sqrt{\frac{2}{\pi}}\frac{x(t^x_{max})}{\dot{x}_{max}}. \quad (23)$$

Thus, the results of MD simulation are in qualitative agreement with the assumptions about the nucleation process made in [7, 42].

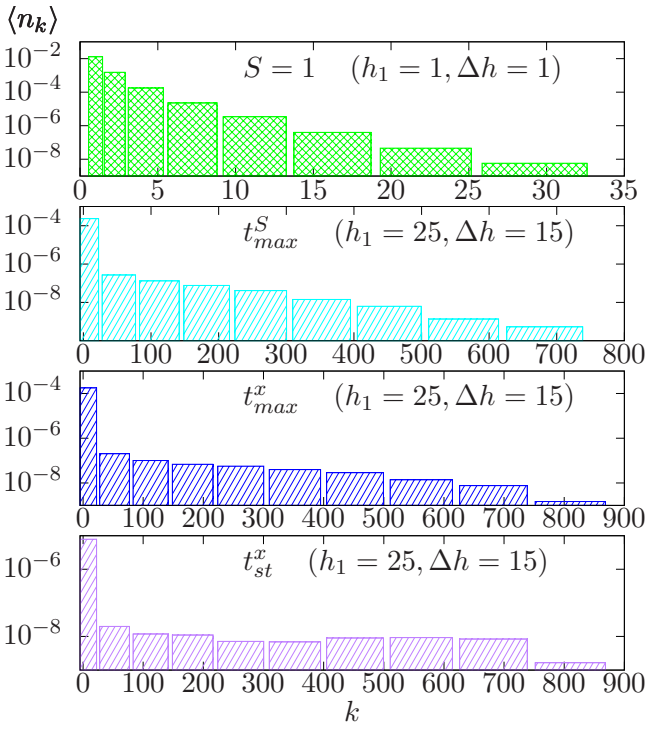

Fig. 4. Distribution of clusters over size n_k at times $S = 1$, t^S_{max}, t^x_{max} and t^x_{st} (see the legend; the values of the parameters h_1 and Δh of the moving average (24) are given in brackets). $\xi = 10^{-5}, n_{v0} = 3/130$

Fig. 4 shows the distribution of clusters by size at different points in time. To construct the distribution, we used a moving average with variable width h

$$\langle n_k \rangle = \sum_{i=k-h_k}^{k+h_k} \frac{n_i}{2h_k+1}; \quad h_k = h_{k-1} + \Delta h. \tag{24}$$

It is evident from Fig. 4 that in the equilibrium state $S = 1$ the cluster size distribution corresponds to formulas (4)–(6). At $t = t^S_{max}$, the maximum cluster size in the system increases sharply due to the growth of supercritical clusters, reaching an almost macroscopic value. At $t = t^x_{max}$, the cluster growth continues, and their spectrum becomes almost flat in a wide range of k, and at $t = t^x_{st}$, a maximum is noticeable in the region of large clusters. In general, such a picture also corresponds to the ideas of [7, 42].

4. KINETICS OF EXPLOSIVE NUCLEATION

The purpose of this section is to extend the analytical approach to the description of the kinetics of non-stationary nucleation [7, 42] to the case of non-ideal vapor with the equation of state (8). The growth rate of a droplet is determined by the difference in the fluxes of condensing ψ and evaporating particles ϕ:

$$\frac{1}{\Sigma}\frac{dk}{dt} = \psi - \phi, \tag{25}$$

where $\Sigma = 4\pi r_\ell^2 \left[k_0(k)(\eta^{-1}-1)+k\right]^{2/3}$ is the total surface area of the cluster [21]. Since it is possible to write with sufficiently high accuracy [21] $\sum_{k=1}^{\infty} k^{1/2} n_k = n_1 Z^{-3/2} = n_{vs} S Z_s^2 Z^{-3/2}$, then

$$\begin{aligned} &= \sum_{k=1}^{\infty} k n_k \frac{v_k}{4} = \frac{v}{4}\sum_{k=1}^{\infty} k^{1/2} n_k \\ &= \frac{v}{4} n_{vs} S Z_s^2 Z^{-3/2}, \end{aligned} \tag{26}$$

where $v_k = v k^{-1/2}$ is the thermal velocity of a cluster containing k particles. We find the expression for the evaporating flow from the condition of equality of both flows on the saturation line

$$\phi = \Big|_{S=1} = \frac{v}{4} n_{vs} Z_s^{1/2}. \tag{27}$$

It is easy to verify that for supercritical clusters, the ratio $\left[k_0(k)\left(\eta^{-1}-1\right)+k\right]^{2/3} \Big/ k^{2/3}$ is equal to 0.3 for $k = 300$ and 0.1 for $k = 1000$. This allows us to write the cluster growth rate in a simplified form

$$\begin{aligned} \frac{dk}{dt} &= \frac{Z^{1/2} - Z^2 Z_s^{-3/2} S^{-1}}{(\pi n_v v r_\ell^2)^{-1}} \\ &\times \left[k_0(k)\left(\eta^{-1}-1\right)+k\right]^{2/3} \simeq k^{2/3}\frac{l}{\tau}, \end{aligned} \tag{28}$$

where $l = Z^{1/2} - Z^2 Z_s^{-3/2} S^{-1}$, $\tau = (\pi n_v v r_\ell^2)^{-1}$. By integrating this expression, we obtain the number of particles in the cluster formed at the time t' by the time t [42]:

$$k^{1/3}(t,t') = g_{TPM}^{1/3}(t') + (l/3\tau)(tt'). \tag{29}$$

The degree of condensation $x = 1 - n_v/n_{v0}$ is determined by the integral [7]

$$x = \int_0^t k(t,t') I(t') dt', \tag{30}$$

where

$$\dot{x} = I(t) g_{TPM}(t) + \int_0^t \frac{dk(t,t')}{dt} I(t') dt'. \tag{31}$$

Further, we will neglect the first terms in the expressions (29) and (31) similarly to [42], which is valid for a sufficiently high cluster growth rate

$$P_1 = \tau g_{TPM}^{1/3} / \Delta t_m l \ll 1 \tag{32}$$

and low rate of change of the supersaturation

$$P_2 = \Delta t_m/\Delta t_S \ll 1. \tag{33}$$

Here, Δt_m and Δt_S are the characteristic duration of explosive condensation and the time of supersaturation change, respectively. The use of the steady-state nucleation rate in (30) and (31) is justified if Δt_m is much greater than the relaxation time of the small cluster size spectrum Δt. This condition can be written as [21]

$$P_3 = \frac{\Delta t}{\Delta t_m} = \frac{9\tau\nu}{16\Delta t_m}\frac{Tg_{TPM}^{2/3}}{Z_s^2\sigma r_\ell^2} \ll 1. \tag{34}$$

The fulfillment of conditions (32), (33) and (34) will be considered in Section 5.1.

Expressing supersaturation through the degree of supercooling $S(t) = \exp[q\theta(t)/T]$, similarly to [7, 42] we expand the nucleation rate in t in the vicinity of the point t_{max}^S, where the supersaturation reaches a maximum, neglecting the time dependence of all quantities except S and θ. Then for the nucleation rate $I_{TPM}(t)$ (9) in the TPM, we obtain

$$\begin{aligned} &I_{TPM}(t) = I_m e^{-\omega(\theta_m-\theta)},\\ &\omega = \frac{32\pi\sigma^3}{3n_\ell^2 q^2 T\theta_m^2}\left(3\gamma_{g_{TPM}} - 2\right),\\ &\theta(t) = \theta_m - \alpha(t-t_{max}^S)^2, \quad \alpha = -\frac{1}{2}\frac{d^2\theta}{dt^2}, \end{aligned} \tag{35}$$

where $I_m = I_{TPM}(t_{max}^S)$ is the maximum value of the nucleation rate. For the nucleation rates given by expressions (10) (CNT) and (13) (SCCNT) in (35), it is sufficient to set $\omega = 32\pi\sigma^3/3n_\ell^2q^2T\theta_m^2$. This makes it possible to integrate expressions (30) and (31) [42]:

$$x = \frac{l^3 I_m}{54\tau^3\alpha^2\omega^2}, \quad \dot{x} = \frac{l^3 I_m}{36\tau^2}\sqrt{\frac{\pi}{\alpha^3\omega^3}}, \tag{36}$$

$$\ddot{x} = \frac{l^3 I_m}{9\tau^3\alpha\omega}. \tag{37}$$

The mass balance equation can be written as

$$n_v = (1-x)n_{v0}. \tag{38}$$

Rewriting (19) as

$$(1-\kappa S)^2\,\dot{S}_\rho = (1-\kappa)^2 S \tag{39}$$

and neglecting the time dependence of κ we differentiate (39) with respect to time:

$$Z^2\dot{S}_\rho - 2\kappa Z\dot{S}S_\rho = Z_s^2\dot{S}. \tag{40}$$

Hence, we find that at the extremum point S, both derivatives are equal to zero:

$$\dot{S}_\rho = \dot{S} = 0. \tag{41}$$

Differentiating (40) again with respect to time, we obtain at $t = t_{max}^S$

$$(\kappa S-1)^2\ddot{S}_\rho + 2\kappa S_\rho(\kappa S-1)\ddot{S} = (\kappa-1)\ddot{S}, \tag{42}$$

where

$$\ddot{S}_\rho = \left(\frac{2}{1-\kappa S} - 1\right)\nu\ddot{S}. \tag{43}$$

Dividing the mass balance equation by n_{vs}, we obtain the expression

$$x = 1 - \frac{S_\rho}{\tilde{S}_\rho}, \quad \tilde{S} = \frac{n_{v0}}{n_{vs}}, \tag{44}$$

differentiation of which with respect to time taking into account the condition $\dot{S} = 0$ and the dependence $n_{vs} = n_0 e^{-q/T}$ (20) allows one to write

$$\dot{x} \simeq -\frac{S_\rho}{\tilde{S}}\frac{q\dot{T}}{T^2} = (x-1)\frac{q\dot{T}}{T^2}. \tag{45}$$

Differentiating (44) twice with due regard for (33) we find that for $t = t_{max}^S$,

$$\ddot{x} \simeq -\frac{\ddot{S}_\rho}{\tilde{S}}. \tag{46}$$

Neglecting the rate of change of temperature compared to the rate of change of S_ρ from the definition of the degree of supercooling θ, we obtain after differentiation

$$\dot{\theta} \simeq \frac{T}{q}\frac{\dot{S}}{S}, \quad \dot{S} = \frac{q}{T}S\dot{\theta}. \tag{47}$$

By repeatedly differentiating this expression at the point where $\dot{S} = 0$ we obtain taking into account (35)

$$\ddot{S} = \frac{q}{T}S\ddot{\theta} = -2\alpha S\frac{q}{T}. \tag{48}$$

Hence, taking into account (38) and the relationship between $\ddot{S}_\rho$ and $\ddot{S}$ (43) we find at the point $t = t_{max}^S$

$$\ddot{S}_\rho = -2\alpha\frac{q}{T}\left(\frac{2}{1-\kappa S} - 1\right)S_\rho. \tag{49}$$

We substitute this expression into (46) taking into account (44):

$$\ddot{x} = 2\alpha\frac{q}{T}(1-x)\left(\frac{2}{1-\kappa S} - 1\right). \tag{50}$$

Taking into account (37) we finally write

$$\alpha = \sqrt{\frac{1}{18}\frac{l^3}{\tau^3}\frac{I_m T}{\omega q(1-x)}\left(\frac{2}{1-\kappa S}-1\right)^{-1}}. \qquad (51)$$

From (35), it follows that the time of action of the source is

$$\Delta t_m = \frac{1}{\sqrt{\alpha\omega}}, \qquad (52)$$

and the supersaturation change time is $\Delta t_S = \sqrt{T/2\alpha q}$. The number density of formed droplets at the moment $t = t^S_{max}$ is found using (35) [42]

$$n_d = \int\limits_{-\infty}^{\infty} I\,dt \approx \sqrt{\pi} I_m \Delta t_m, \quad I_m = I(\theta_m). \qquad (53)$$

Since we consider the droplets formed in the process of "condensation explosion" and the nucleation rate I is almost zero before and after this stage, the integration limits in (53) can be extended to infinity. Taking into account the assumed symmetry of $I(t)$ with respect to time t^S_{max} (see (35)) we can conclude that the droplet number density at the moment t^S_{max} is $n_d/2$.

The set of equations that determines the quantities characterizing the "condensation explosion" is obtained by substituting (45) into (36):

$$\begin{gathered} x(t) = \frac{l^3 I_m(x,t)}{54\tau^3\alpha^2\omega^2}, \\ \frac{l^3 I_m(x,t)}{36\tau^2}\sqrt{\frac{\pi}{\alpha^3\omega^3}} = [x(t)-1]\,\frac{q\dot{T}}{T^2}. \end{gathered} \qquad (54)$$

This system is transcendental and can be solved by the convergence method with respect to the unknowns x and t.

5. RESULTS OF THE NUCLEATION KINETICS CALCULATIONS

5.1. Nucleation in the Lennard-Jones system

To solve the system of equations (54), interpolation dependences (20) were used, the TPM parameters δ and λ were borrowed from [21]. For subsequent comparison of the analytical results with the results of numerical simulation, the condition $n_{v0} = \text{const}$ and the linear law of temperature change $T = 1.3 - \xi t$ were used. The system of equations (54) was solved using expressions for the nucleation rate in the TPM, CNT, and SCCNT models (formulas (9), (10), and (13); the quantities corresponding to these models are denoted in what follows by the subscripts TPM, CNT, and SCCNT). In this case, in the calculations using the CNT and SCCNT models, the non-ideality of the vapor was not taken into account, and thus, in all formulas in Section 4 it was assumed that $\kappa = 0$, $Z = 1$, $S_\rho = S$.

The calculation results for the TPM and CNT models are shown in Figs. 5–8. It is evident that the TPM predicts lower supersaturations at the point of maximum supersaturation at a high cooling rate compared to the CNT (Fig. 5). A characteristic feature of the CNT is the absence of a solution at $\xi \gtrsim 10^{-5}$, which indicates the boundary of the lability region. The same is evidenced by the peculiarity of T_{CNT} in Figs. 6 and 10, as well as the peculiarity of S_ρ in Fig. 11. At a fixed cooling rate, the peculiarities of S, g, and T for the CNT manifest themselves at low densities, while they are absent for the TPM (Figs. 7 and 8). According to the TPM, the "condensation explosion" is in the metastable region and is characterized by the absence of singularities, which corresponds to the MD simulation data (Sec. 5.2). For the CNT, on the contrary, there is a singularity of the critical size ($g \to 0$ at $S \to \infty$), which can be seen in Fig. 5, and the values $g < 10$ are reached, at which the cluster clearly cannot be considered a macroscopic drop. The critical size in the TPM is much larger than in the CNT. In Fig. 6, it is also clearly visible that with an increase in ξ, Z falls, and the vapor differs significantly from the ideal one.

Figures 7 and 8 illustrate the results of calculations in the parameter region inaccessible to numerical simulation (low cooling rate and total particle number density). It is interesting to note that the vapor becomes significantly non-ideal (small Z) not only at high total particle number density n_{v0}, but also at low number density (Fig. 8), which is a consequence of the sharp increase in supersaturation.

The fulfillment of the criteria of the approximations (32)–(34) used in deriving the system of equations (54) is analyzed in Fig. 9. To calculate the values of the criteria as functions of ξ, all variables were taken at the point of maximum supersaturation $t = t^S_{max}$, i.e. the solution of the system (54) was used; Δt_m was found using the formula (52).

It is evident that all criteria are violated at sufficiently large ξ, and the criterion (34) is violated first of all, i.e. non-stationarity of the rate of formation of supercritical nuclei is manifested. In addition, the applicability of the considered analytical model is limited by too small values of $Z < 0.5$, as can be seen from Figs. 6 and 8. Criteria (32) and (33) are fulfilled quite well in the entire considered range of parameter values.

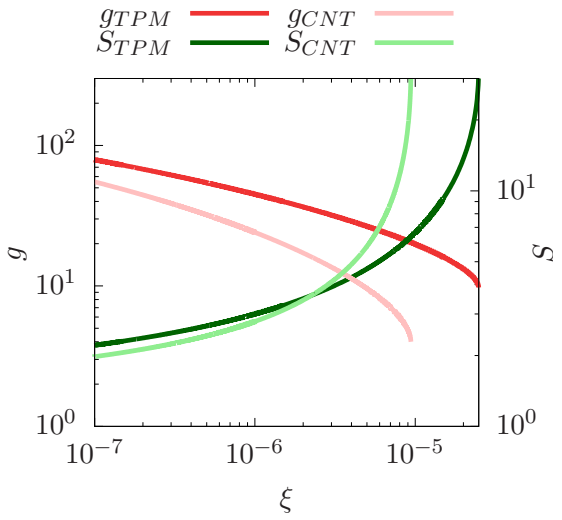

Fig. 5. Dependence of the critical size and the supersaturation on the cooling rate at $t = t^S_{max}$ and $n_{v0} = 3/130$

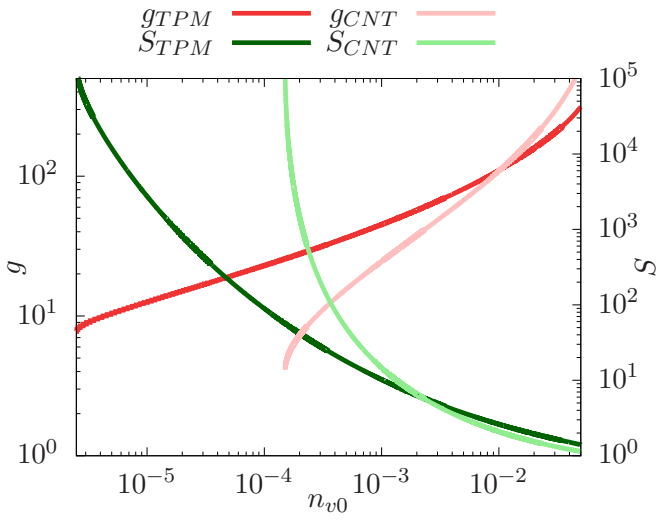

Fig. 7. Dependence of the critical size and the supersaturation on the total number density of particles at $\xi = 10^{-10}$

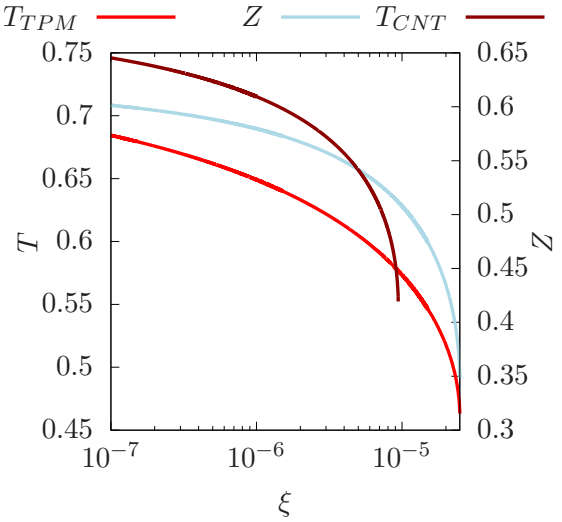

Fig. 6. Values of T and Z at $t = t^S_{max}$ as functions of the cooling rate; $n_{v0} = 3/130$

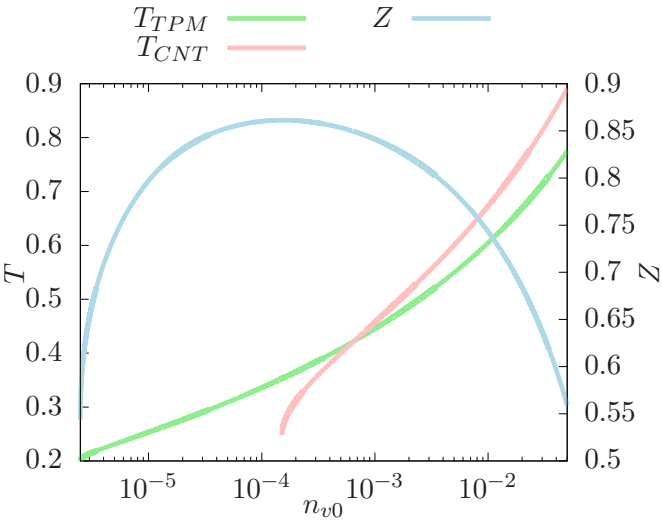

Fig. 8. Dependence of Z and T on the total number density of particles at $\xi = 10^{-10}$

5.2. Comparison of MD simulation and analytical calculations results

The parameters of the "condensation explosion" obtained from the MD simulation data at $t = t^S_{max}$ are compared with the results of analytical calculations for different total vapor number densities in Fig. 10–12. As can be seen from Fig. 10, the TPM model qualitatively and quantitatively corresponds to the numerical simulation, the CNT does not correspond even qualitatively, and the SCCNT qualitatively correctly reproduces the trends of the dependencies, but gives significantly overestimated temperature values. For the value of S_ρ, the correspondence of the TPM model turns out to be quantitatively worse, but it is clear that this model still best describes the results of the MD simulation (Fig. 11). In this case, the SCCNT results in greatly underestimated values of S_ρ. The discrepancy between the TPM and the numerical simulation results may be due to factors such as insufficient accuracy of the vapor density estimate, the proximity of the parameters of the simulated system to the spinodal decomposition region, and

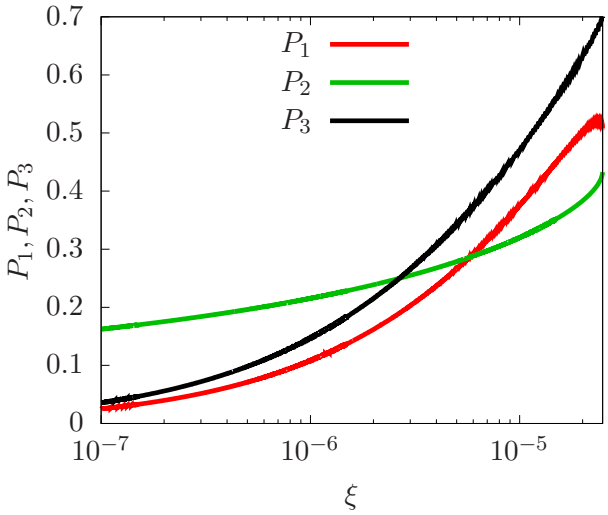

Fig. 9. Fulfillment of the validity criteria of the approximations used (32)–(34) at different cooling rates for $n_{v0} = 3/130$

going beyond the applicability of the theory at too small Z. The cluster number density at the point of maximum supersaturation $n_d/2$ (Fig. 12), calculated using the TPM (formula (53)), also demonstrates satisfactory agreement with the numerical results, while the SCCNT yields significantly overestimated values. The accuracy of the CNT here is comparable to the TPM, but the latter describes the trend of the simulation results better. Note the rather weak dependence of $n_d/2$ on the total vapor number density, which is manifested both in the MD simulation results and in the analytical calculation.

The significant discrepancy between the TPM and MD at a single point at $\xi = 10^{-6}$ (Fig. 12a) may be explained by inaccuracy of the MD simulation, since at low cooling rates, the number density of critical-size clusters is also small, so that for such values of ξ the statistics for estimating $n_d/2$ could be insufficient, which as is known leads to an overestimation of the numerical estimate. It is possible that to refine this value it is necessary to increase the number of particles in the computational cell.

When performing calculations using CNT and SCCNT, the non-ideality of vapor was not taken into account, so it is of interest to estimate the compressibility factor that results from using these models. For this, we use the relation

$$Z \simeq \sum_{k=1}^{10} \bar{n}_k \left(\sum_{k=1}^{10} k \bar{n}_k \right)^{-1}, \qquad (55)$$

where $\bar{n}_k$ is taken in accordance with the CNT and SCCNT models (see section 2). Then for $n_{v0} = 3/130$ and $\xi = 10^{-5}$, which corresponds to the parameter values in Fig. 10–12, we obtain $Z \simeq 0.16$ for CNT and SCCNT (the close values of Z are explained by the fact that at the point of maximum supersaturation for SCCNT the temperature is higher than for CNT, but the lower supersaturation compensates for the difference in values). From this, we can conclude that both models without taking into account the non-ideality of the vapor are internally inconsistent. In CNT and SCCNT, not taking into account the non-ideality partially compensates for the inaccurate accounting of the size dependence of the cluster surface tension, which can bring the results of the TPM and these models closer together.

Thus, it can be concluded that the TPM as a whole best describes the results of MD simulation.

5.3. Nucleation in silicon dioxide vapor

It is possible to verify that taking into account the equation of state of condensing vapor is essential not only for the Lennard-Jones system by treatment of nucleation in SiO_2 vapor. The choice of this substance is connected firstly with the fact that analytical calculations for it using CNT have already been made in [42] and secondly with the already mentioned problem of the formation and evolution of regolith.

Neglecting the effect of vapor pressure changes on the nucleation kinetics, for calculations we can approximately set $n_{v0} = \chi p/T$, where χ is the fraction of SiO_2 molecules in the gas flow, and the pressure p and temperature T of this flow are taken at the point of maximum supersaturation. The thermophysical quantities characterizing silicon oxide and its vapor, as well as the parameters of the gas flow, are borrowed from [42], and for calculations according to the TPM model, the same values were taken as for the Lennard-Jones system: $\delta = -0.07$ and $\lambda = 2.1$.

The calculation results shown in Fig. 13 are qualitatively similar to those for the Lennard-Jones system; however, unlike the latter, with increasing cooling rate a sharp drop in Z precedes entering the lability region. Therefore, on the side of large values, the range of ξ is limited by $Z \sim 0.1$, at which the calculated value of the critical size according to the CNT becomes negative. Similar to the Lennard-Jones system, the calculation according to the CNT leads to much higher values of S and, accordingly, low g. Note that for the CNT at $\xi = 1.4 \cdot 10^3$ K/s, which is the cooling rate in [42], the values of the parameters

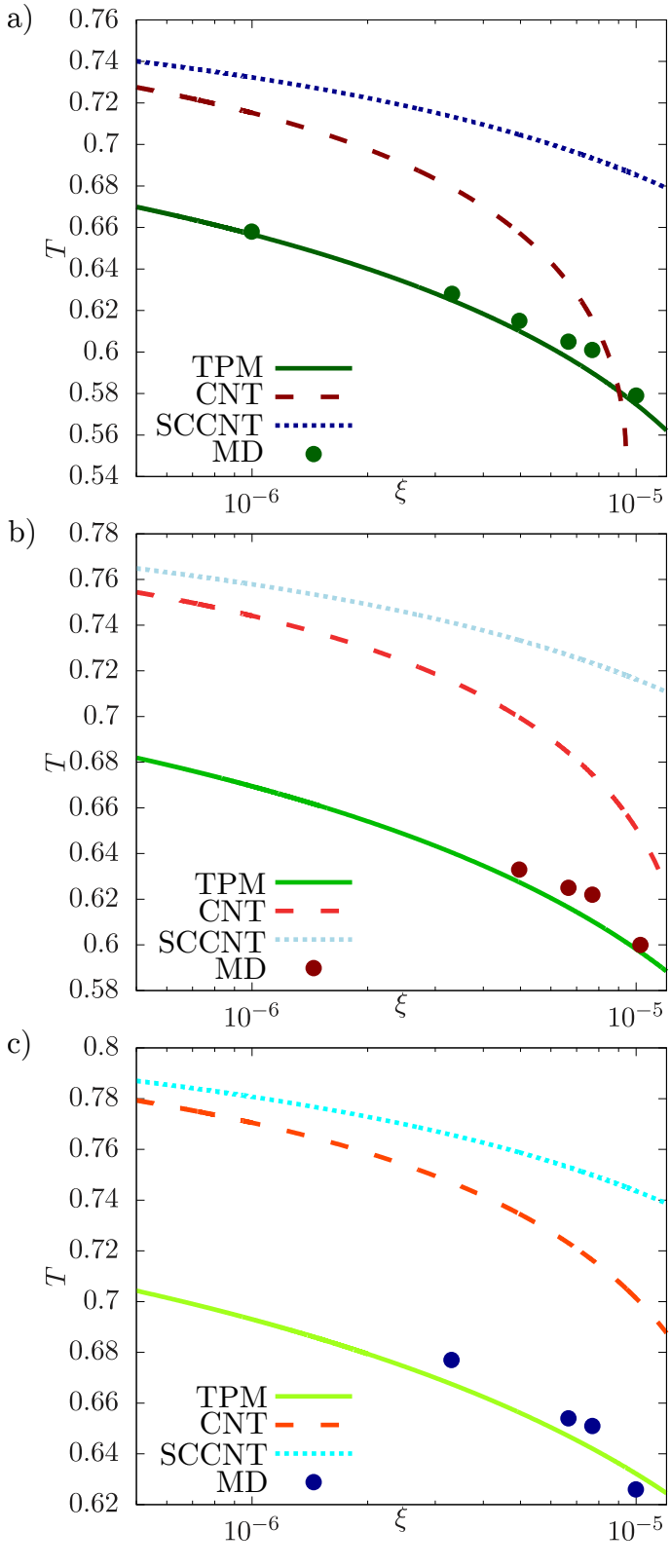

Fig. 10. Comparison of temperature at $t = t^S_{max}$ as a function of ξ calculated using the analytical models CNT, SCCNT and TPM (curves) and obtained from MD simulation data (points) (see legend). a) $n_{v0} = 3/130$, b) $n_{v0} = 3.5/130$, c) $n_{v0} = 4/130$

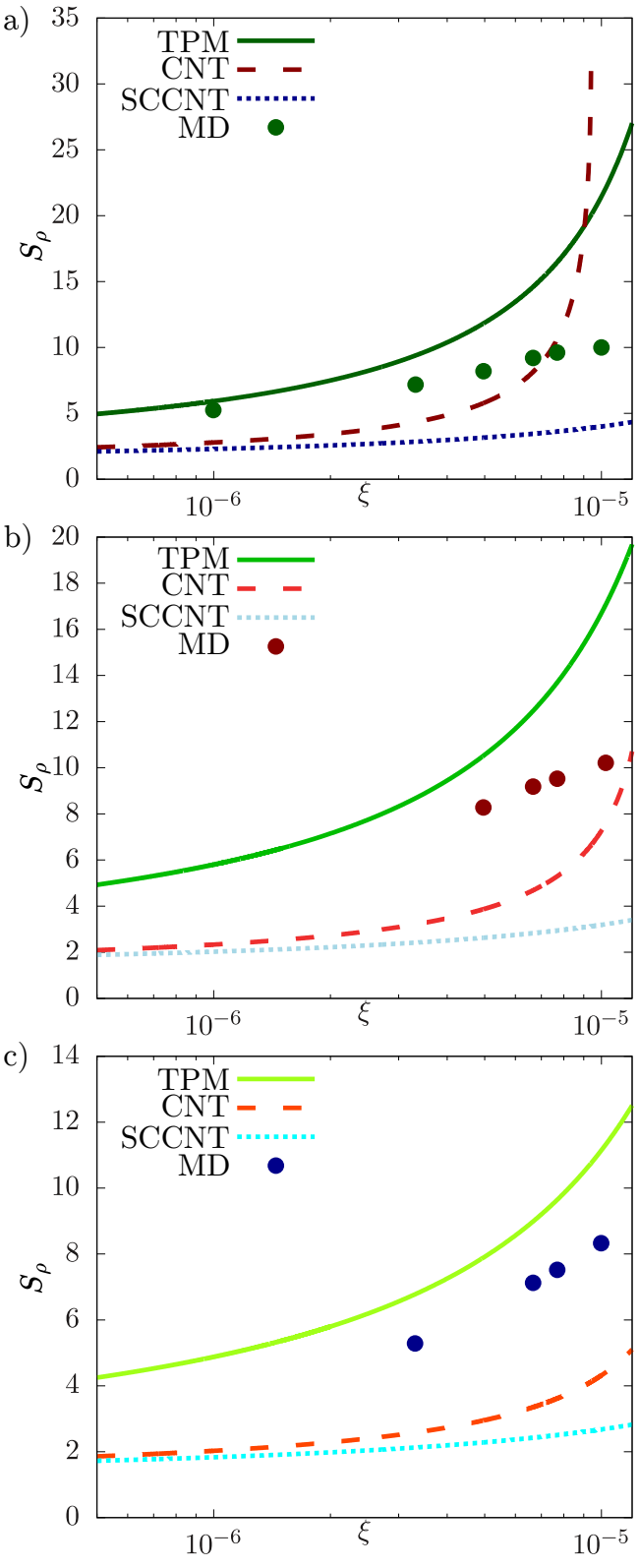

Fig. 11. Same as in Fig. 10, for the value S_ρ

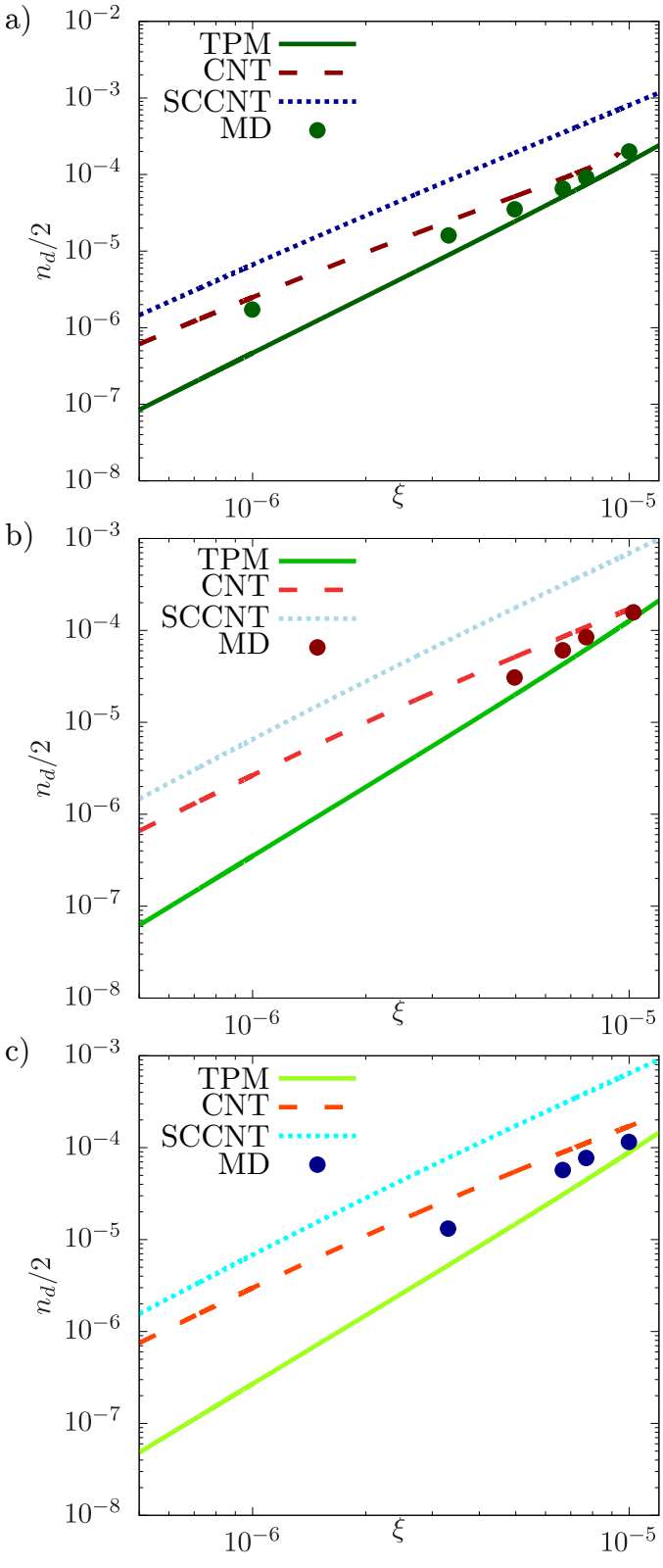

Fig. 12. Same as in Fig. 10, for the value $n_d/2$

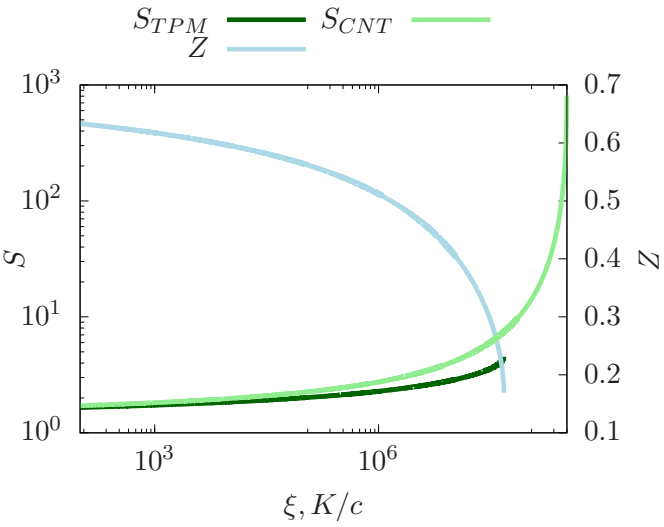

Fig. 13. Dependence of the supersaturation and the compressibility factor on the cooling rate ξ, calculated for the CNT and TPM models for the conditions [42]

at the point of maximum supersaturation obtained in this work are reproduced.

Note also the lack of similarity between the results obtained for SiO_2 and the Lennard-Jones system even when using dimensionless quantities. For example, if we take $q/5$ and $n_\ell^{-1/3}$ as the units of energy and length for SiO_2, respectively, then we obtain that the sharp drop in Z in Fig. 13 corresponds to a dimensionless cooling rate of the order of 10^4. This is more than eight orders of magnitude greater than the corresponding value for the Lennard-Jones system (Fig. 6).

6. CONCLUSION

In this paper, the problem of non-stationary nucleation during the vapor-liquid phase transition is considered. An analytical approach to describing the kinetics of this process is developed, taking into account the non-ideality of the condensing vapor. The previously obtained equation of state of the vapor is used, which assumes that its non-ideality is due to the presence of the lightest clusters containing less than 10 monomers. The number density of such clusters is high not only at high total vapor number densities, but also at low vapor densities but high supersaturations. In such states, the vapor is strongly non-ideal, which significantly affects the rate of formation of supercritical clusters. A self-consistent analytical solution to the problem of nucleation kinetics of rapidly cooled vapor is found, based on

three models of small clusters, CNT, SCCNT, and TPM. The latter correctly takes into account the dependence of the work of cluster formation on its size. The results of calculations using these models lead to qualitatively different results, namely, they indicate the existence of such a region of system parameters where the TPM predicts a metastable state at the point of maximum supersaturation of the vapor, while the CNT indicates a state of its lability.

For numerical simulation of the process under consideration, the molecular dynamics method for the Lennard-Jones system was used. A method for numerical determination of the main parameters characterizing the "condensation explosion", supersaturation and degree of condensation, as well as the time of the onset of nucleation was proposed. The spectrum of sizes of clusters present in the vapor was determined. It was shown that the evolution of all quantities, in particular, the bell-shaped dependence of the degree of supersaturation on time, fully corresponds to that assumed in the analytical model.

Comparison of the MD simulation results and analytical calculations shows that the calculation using the TPM best corresponds to the simulation results; there is satisfactory quantitative correspondence at the point of maximum supersaturation of its value, the temperature of the system and the number density of supercritical clusters. Thus, simulation of non-stationary nucleation as a whole was carried out, during which the rate of formation of supercritical clusters can be considered quasi-stationary. Satisfactory agreement between the MD simulation results and analytical calculations allows us to claim the model to be correct and accuracy of the results obtained on its basis, to be sufficient, and also to assume that the model yields reasonable results outside the range of parameters available for MD simulation.

Analytical calculations performed for the nucleation of silicon dioxide also demonstrate a significant difference in the results using the TPM and the CNT. At the point of maximum supersaturation, the vapor turns out to be even more non-ideal than in the Lennard-Jones system. This indicates that potentially the non-ideality of the vapor in the "condensation explosion" is its universal property, independent of either the substance or the cooling conditions of the system.

Thus, when considering the kinetics of non-stationary nucleation, it is necessary to take into account not only the dependence of the work of formation of a critical cluster on its size, but also the non-ideality of the condensing vapor. This non-ideality can be taken into account using the equation of state proposed in the work, which should be applicable to any substance in the metastable region.

REFERENSES

1. V. E. Bondybey, J. H. English, J. Chem. Phys. **74**, 6978 (1981).

2. T. Masubuchi, J. F. Eckhard, K. Lange et al, J. Chem. Phys. **89**, 023104 (2018).

3. S. I. Anisimov, B. S. Luk'yanchuk, Phys. Usp. **45**, 293 (2002).

4. B. Chimier, V. T. Tikhonchuk, Phys. Rev. B **79**, 184107 (2009).

5. M. E. Povarnitsyn, T. E. Itina, P. R. Levashov, and K. V. Khishchenko, Phys. Chem. Chem. Phys. **15**, 3108 (2013).

6. N. A. Inogamov, V. V. Zhakhovsky, V. A. Khokhlov, JETP **154**, 92 (2018).

7. Yu. P. Raizer, JETP **37**, 1741 (1959).

8. Ya. B. Zeldovich, JETP **12**, 525 (1942).

9. M. Volmer, A. Weber, Z. Phys. Chem. **199**, 277 (1926).

10. R. Becker, W. Döring, Ann. Phys. **416**, 719 (1935).

11. J. H. ter Horst, D. Kashchiev, J. Chem. Phys. **123**, 114507 (2005).

12. E. N. Chesnokov, L. N. Krasnoperov, J. Chem. Phys. **126**, 144504 (2007).

13. M. Horsch, J. Vrabec, H. Hasse, Phys. Rev. E **78**, 011603 (2008).

14. I. Napari, J. Julin, H. Vehkamäki, J. Chem. Phys. **133**, 154503 (2010).

15. A. S. Abyzov, J. W. P. Schmelzer, A. A. Kovalchuk et al, J. Non-Cryst. Solids **356**, 2915 (2010).

16. G. Wilemski, J. Chem. Phys. **103**, 1119 (1995).

17. R. H. Heist, H. He, J. Chem. Phys. **23**, 781 (1994).

18. E. Ruckenstein, Y. S. Djikaev, Adv. Colloid Interface Sci. **118**, 51 (2005).

19. J. D. Gunton, J. Stat. Phys. **95**, 903 (1999).

20. D. I. Zhukhovitskii, J. Chem. Phys. **101**, 5076 (1994).

21. D. I. Zhukhovitskii, D. I. J. Chem. Phys. **144**, 184701 (2016).

22. D. I. Zhukhovitskii, J. Chem. Phys. **110**, 7770 (1999).

23. D. I. Zhukhovitskii, JETP **109**, 839 (1996).

24. D. I. Zhukhovitskii, JETP **113**, 181 (1998).

25. D. I. Zhukhovitskii, JETP **121**, 396 (2002).

26. D. I. Zhukhovitskii, J. Chem. Phys. **142**, 164704 (2015).

27. D. I. Zhukhovitskii, V. V. Zhakhovsky, J. Chem. Phys. **152**, 224705 (2020).

28. P. R. ten Wolde, D. Frenkel, J. Chem. Phys. **109**, 9901 (1998).

29. S. Toxvaerd, J. Chem. Phys. **119**, 10764 (2003).

30. K. K. Tanaka, K. Kawamura, H. Tanaka et al, J. Chem. Phys. **122**, 184514 (2005).

31. J. Wedekind, J. Wölk, D. Reguera et al, J. Chem. Phys. **127**, 154515 (2007).

32. K. K. Tanaka, H. Tanaka, T. Yamamoto et al, J. Chem. Phys. **134**, 204313 (2011).

33. I. Napari, J. Julin, H. Vehkamäki, J. Chem. Phys. **131**, 244511 (2009).

34. V. G. Baidakov, A. O. Tipeev, K. S. Bobrov et al, J. Chem. Phys. **132**, 234505 (2010) .

35. J. Diemand, R. Angélil, K. K. Tanaka et al, J. Chem. Phys. **139**, 074309 (2013).

36. K. K. Tanaka, J. Diemand, R. Angélil et al, J. Chem. Phys. **140**, 194310 (2014).

37. R. Angélil, J. Diemand, K. K. Tanaka et al, J. Chem. Phys. **143**, 064507 (2015).

38. K. J. Oh, X. C. Zeng, J. Chem. Phys. **114**, 2681 (2001).

39. J. Merikanto, H. Vehkamäki, E. Zapadinsky, J. Chem. Phys. **121**, 914 (2004).

40. A. V. Neimark, A. Vishnyakov, J. Phys. Chem. **109**, 5962 (2005).

41. J. Merikanto, E. Zapadinsky, H. Vehkamäki, J. Chem. Phys. **125**, 084503 (2006).

42. D. I. Zhukhovitskii, A. G. Khrapak, I. T. Yakubov, TVT **21**, 982 (1983).

43. D. I. Zhukhovitskii, A. G. Khrapak, I. T. Yakubov, TVT **21**, 1197 (1983).

44. J. L. Katz, M. Blander, J. Colloid Interface Sci. **42**, 496 (1973).

45. A. Laaksonen, I. J. Ford, M. Kulmala, Phys. Rev. E**49**, 5517 (1994).

46. W. Band, J. Chem. Phys. **7**, 324 (1939).

47. W. Band, J. Chem. Phys. **7**, 927 (1939).

48. D. I. Zhukhovitskii, Journal of Physical Chemistry, **67**, 1962 (1993).

49. A. P. Thompson, H. M. Aktulga, R. Berger et al., Comp. Phys. Comm. **271**, 108171 (2022).

50. S. I. Anisimov, D. O. Dunikov, V. V. Zhakhovskii et al, J. Chem. Phys. **110**, 8722 (1999).